Experimental bilocality violation without shared reference frames

Francesco Andreoli,[1] Gonzalo Carvacho,[1] Luca Santodonato,[1] Marco Bentivegna,[1] Rafael Chaves,[2] and Fabio Sciarrino[1,*]

[1]*Dipartimento di Fisica–Sapienza Università di Roma, P.le Aldo Moro 5, I-00185 Roma, Italy*

[2]*International Institute of Physics, Federal University of Rio Grande do Norte, 59070-405 Natal, Brazil*

(Received 13 January 2017; published 9 June 2017)

Nonclassical correlations arising in complex quantum networks are attracting growing interest, both from a fundamental perspective and for potential applications in information processing. In particular, in an entanglement swapping scenario a new kind of correlations arise, the so-called nonbilocal correlations that are incompatible with local realism augmented with the assumption that the sources of states used in the experiment are independent. In practice, however, bilocality tests impose strict constraints on the experimental setup and in particular to the presence of shared reference frames between the parties. Here, we experimentally address this point showing that false positive nonbilocal quantum correlations can be observed even though the sources of states are independent. To overcome this problem, we propose and demonstrate a scheme for the violation of bilocality that does not require shared reference frames and thus constitutes an important building block for future investigations of quantum correlations in complex networks.

DOI: 10.1103/PhysRevA.95.062315

I. INTRODUCTION

Bell's theorem [1] shows that quantum-mechanical correlations can violate the constraints imposed by any classical explanation based on local realism, the phenomenon known as Bell nonlocality. To prove the emergence of quantum nonlocal correlations it is sufficient to consider a very simple causal structure, where distant parties perform different measurements on their shares of a quantum entangled system. The classical description of this scenario defines the so-called *local hidden variables* (LHV) models, which have been widely studied [2], up to the recent loophole-free experimental tests [3–5] that have conclusively ruled out such causal models as a possible explanation for quantum phenomena.

Recently, generalizations of Bell's theorem for more complex causal structures have attracted growing attention [6–16]. Exploring the incompatibility of quantum and classical descriptions in more general scenarios is of fundamental importance to understand the role of causality within quantum theory [17–24] and promises novel routes for quantum information processing in quantum networks of increasing complexity. A new and important feature of such networks, as for example in quantum repeaters [25], is the fact that typically the correlations between the distant parties are mediated by several independent sources of quantum states. The simplest example is an entanglement swapping experiment [26], where a central node (Bob) shares two independent quantum states with two other uncorrelated parties (Alice and Charlie) and by jointly measuring the particles in his possession can generate entanglement between them. A precise classical description of this experiment must include the independence of the sources, which introduces the so-called bilocality assumption in Bell's theorem [6,7]. Importantly, as shown in recent experiments [27,28], there are correlations that admit a LHV model but nonetheless are incompatible with the bilocality assumption.

In this work we focus on related aspects of the bilocality scenario. First, we experimentally verify a route to certify nonbilocal quantum correlations, performing only single qubit operations, as opposed to the results in [27,28] that require entangled measurements. We then investigate the importance of the independence between Alice and Charlie, in particular in relation to the necessity of sharing a reference frame (RF) between the parties [30–35]. While in a usual Bell test shared RFs do not change the causal structure under test, this is no longer true in a bilocality test since they can establish hidden correlations between parties that are assumed to be independent. We experimentally verify this point by showing that nonbilocal correlations may arise even though only classical channels are shared between the parties, thus leading to false positive quantumness. We thus study how this independence can be ensured, by proposing and implementing a scheme which violates a bilocality inequality without the need of shared RFs. Our results thus show that bilocality violation is a feasible and reliable method to certify quantum correlations in a tripartite scenario.

II. WITNESSING NONBILOCALITY WITH SEPARABLE MEASUREMENTS

The classical description of a tripartite Bell scenario depends on the precise causal structure under test. In a usual Bell scenario, one assumes that the correlations between all distant parties are mediated by a single common hidden variable, the standard LHV model, which is depicted in Fig. 1(a). However, in a scenario akin to entanglement swapping, the fact that particles are generated in two distinct and separated sources is taken into account by considering two different and causally independent hidden variables λ_1 and λ_2, leading to the definition of a *bilocal hidden variable* (BLHV) model [Fig. 1(b)]. If Alice, Bob, and Charlie measure two possible dichotomic observables each (A_0, A_1, B_0, B_1, C_0, and C_1), any correlation compatible with this model respects the inequality [7]

$$\mathcal{B} = \sqrt{|I|} + \sqrt{|J|} \leqslant 1, \tag{1}$$

*fabio.sciarrino@uniroma1.it

 ©2017 American Physical Society

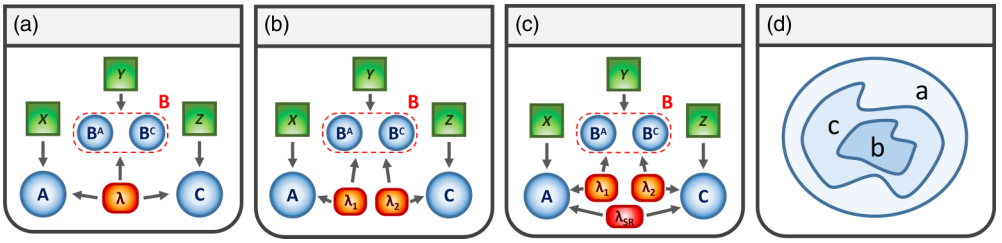

FIG. 1. Directed acyclic graphs [29] representing tripartite causal structures. Nodes represent random variables while arrows represent their causal relations. Blue circles show variables related to measurement outcomes, green squares represent measurement choice inputs, and orange blunt rectangles represent hidden variables. (a) Tripartite LHV model where the central node B is made of two substations B^A and B^C, driven by the same measurement choice y. (b) BLHV model with the two independent hidden variables λ_1 and λ_2 mediating the correlations. (c) Classical representation of the previous scenario when allowing for shared randomness between A and C (red rectangle). (d) Pictorial representation of the structure of the correlations in the three subpanels (a), (b), and (c).

with $I = \frac{1}{4}\sum\langle A_x B_0 C_z\rangle$, $J = \frac{1}{4}\sum(-1)^{x+z}\langle A_x B_1 C_z\rangle$ (summing on $x,z = 0,1$), and where $\langle A_x B_y C_z\rangle = \sum(-1)^{a+b+c} p(a,b,c|x,y,z)$ (summing on $a,b,c = 0,1$).

Imposing the same causal structure to quantum mechanics we can generate correlations violating inequality (1), the so-called nonbilocal correlations that are incompatible with a BLHV model. As experimentally shown in Refs. [27,28] using photons entangled in polarization, a violation of bilocality can be witnessed even when the experimental data is compatible with a LHV model, thus demonstrating a new form of quantum nonlocality. However, these experiments consider a scenario where the central node B is assumed to perform a complete Bell-state measurement with four possible outcomes, something that is impossible with linear optics [36]. In practice this implies that such realizations have to rely on the precise quantum description of the experiment, that is, we have a device-dependent test of nonbilocality. It is then natural to consider whether a device-independent test of bilocality—where we do not have to rely on the precise description of the measurements but only on the empirical data—is possible.

Notably it can be shown that quantum mechanics can exhibit nonbilocal correlations also in cases where all parties only perform single qubit operations (i.e., σ_x, σ_z, σ_y, and linear combinations). Such measurements can be performed with linear optics, then allowing for a device-independent test of bilocality. For instance, inequality (1) is violated if (A,B) and (B,C), respectively, share a pair of photons in a singlet state and perform the following measurements: $A_0 = C_0 = (\sigma_x + \sigma_z)/\sqrt{2}$, $A_1 = C_1 = (\sigma_x - \sigma_z)/\sqrt{2}$, and $B_y = (1-y)(\sigma_x \otimes \sigma_x) + y(\sigma_z \otimes \sigma_z)$ [13,37]. Since all parties only perform single qubit operations this scenario is equivalent to considering outcome B as a function of two individual outcomes B^A and B^C, both driven by the measurement choice Y [Fig. 1(b)].

We experimentally witness quantum nonbilocality exploiting only separable measurements, using a photonic setup where two independent pairs of photons (1-2 and 3-4 in Fig. 2) are generated by a type-II spontaneous parametric down-conversion process (SPDC) in two separated crystals. One photon of each source is then directed to one of two different measurement stations (photon 1 to Alice and photon 4 to Charlie) where polarization analysis is performed by using a half-wave plate (HWP) followed by a polarizing beam splitter (PBS). Photons 2 and 3 instead are separately sent to the two substations B^A and B^C where two polarization analyses are performed, analogously to the ones performed in stations A and C. Within this scheme, we obtain $\mathcal{B} = 1.2712 \pm 0.0042$, witnessing a violation of (1) of almost 65 sigmas.

III. QUANTUM NONBILOCALITY MIMICKED BY SHARED RANDOMNESS

When performing a bilocality test, it is essential to ensure that the experiment actually has the same causal structure as the one depicted in Fig. 1(b). In particular, one has to guarantee that Alice and Charlie do not have access to any shared randomness. At first, this assumption may seem to be straightforwardly ensured by preparing a quantum state in the form $\varrho_{AB} \otimes \varrho_{BC}$, indeed guaranteeing that Alice and Charlie are uncorrelated. However, when performing Bell tests, it is usually necessary to establish a shared RF between the measurement devices [30–35]. While this is generally a practical rather than a fundamental issue, in a bilocality scenario the communication required to establish a RF could also be used to establish undesired correlations between parties that are assumed to be independent. Therefore, in this case, we cannot guarantee that the experimental setup fulfills the bilocality assumption anymore. In fact, as we show next, it is sufficient to allow for

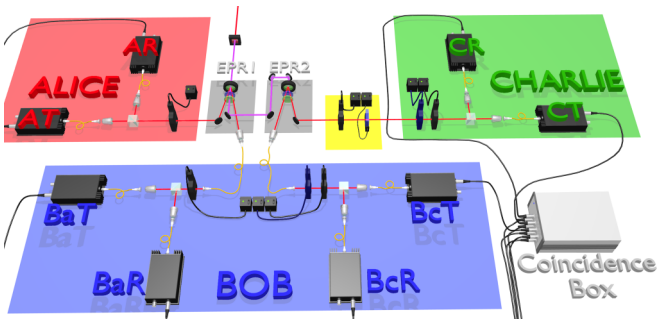

FIG. 2. Experimental setup. Two separated nonlinear crystals (EPR1 and EPR2) generate polarization-entangled photon pairs via a SPDC process. Photons 1 and 4 are directed to Alice's and Charlie's stations, respectively, where the analysis in polarization of a particular observable is performed by using a motorized HWP and a PBS. Photons 2 and 3 are directed to the two different substations B^A and B^C where an analogous analysis is performed.

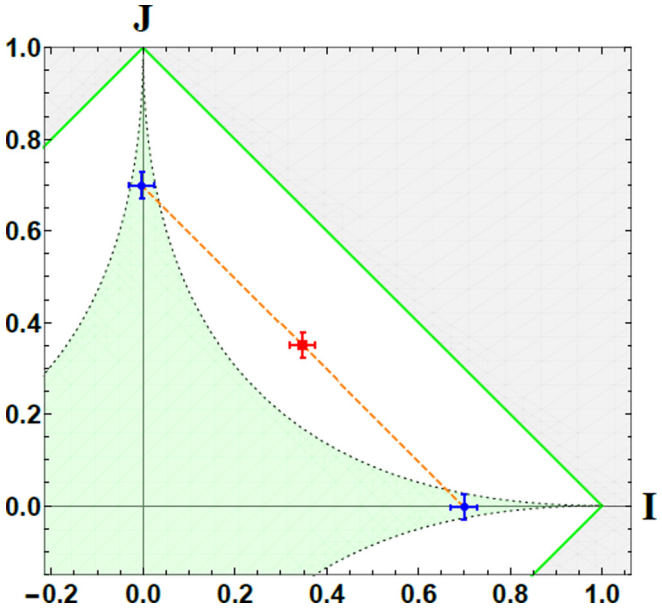

FIG. 3. Nonbilocal correlations from shared randomness. The green shaded area within the dotted lines shows the bilocal set in the I, J plane, while the bold green line bounds the local set (that includes the bilocal one). The blue circle points show the experimental results for a fixed distribution (2), while the red square point represents the equal mixing of these two points (i.e., shared randomness). Error bars are due to Poissonian statistics.

some shared randomness between Alice and Charlie [Fig. 1(c)] to classically simulate nonbilocal correlations.

We experimentally show this phenomenon exploiting two pairs of photons in a state $\varrho_{AB} \otimes \varrho_{BC}$, where $\varrho_{AB} = \varrho_{BC} = \sqrt{v}(|HH\rangle\langle HH| + |VV\rangle\langle VV|)/2 + (1-\sqrt{v})\mathbb{I}/4$ (see Appendix A for state generation details). Both pairs of photons are in a classical mixture of separable states and thus, if the bilocal causal structure [Fig. 1(b)] is imposed, no violation of the inequality (1) should be observed. That is not the case if Alice and Charlie share some underlying correlations, represented in Fig. 1(c) by a binary variable λ_{SR}. Making use of this shared randomness and using the measurement settings $A_0 = A_1 = C_0 = C_1 = \sigma_z$ and $B_0^A = B_0^C = B_1^A = B_1^C = \sigma_z$ we can exactly simulate quantum correlations. To that aim, when $\lambda_{\mathrm{SR}} = 0$ the parties perform a usual bilocality test applying the aforementioned settings. When $\lambda_{\mathrm{SR}} = 1$, Alice and Charlie apply a postprocessing to their outcomes multiplying them by $(-1)^x$ and $(-1)^z$, respectively. This leads to the two probabilities $p_0 \equiv p(a,b,c|x,y,z,\lambda_{\mathrm{SR}} = 0)$ and $p_1 \equiv p(a,b,c|x,y,z,\lambda_{\mathrm{SR}} = 1)$, where

$$p_k = v\tfrac{1}{8}[1 + (-1)^{a+c+b+k(x+z)}] + (1-v)\tfrac{1}{8}. \qquad (2)$$

These two distributions are bilocal for all v. However, using their shared randomness, Alice and Charlie can mix their strategies in a correlated manner and obtain $p(a,b,c|x,y,z) = (p_0 + p_1)/2$, which violate (1) for any $v > 1/2$.

Our experimental results are shown in Fig. 3. The blue circles represent the case of no shared randomness, with the measurement outputs defined by the λ_0 or λ_1 prescriptions. As expected, these points are inside the bilocal set, showing an experimental value of $\mathcal{B} = 0.892 \pm 0.062$, which is compatible with (1) by almost two sigmas. The red square shows how the mixing of these two probabilities gives a nonbilocal point with $\mathcal{B} = 1.180 \pm 0.034$, meaning a bilocality violation of more than five sigmas. This shows that the independent preparation of two quantum states ϱ_{AB} and ϱ_{BC} is not sufficient to justify the bilocality assumption and thus guarantee the observation of truly quantum correlations in this tripartite network.

IV. VIOLATION OF BILOCALITY WITHOUT SHARED REFERENCE FRAMES BETWEEN SOME OF THE STATIONS

In view of this result, any experimental observation of nonbilocality requiring the use of shared RFs (that may generate correlations between Alice and Charlie) is highly unsatisfactory. Thus, to turn the violation of a bilocality inequality into a reliable test of nonclassical behavior it is crucial to ask: is it possible to observe nonbilocal correlations even in the absence of shared RFs? To answer in positive to this question, we consider a few relevant situations. In the following we focus on a scenario where only Alice and Bob share a RF. We describe a scheme allowing for the violation of bilocality in this case as well as an experimental implementation of it. In the next section we also propose a scheme allowing for witnessing nonbilocality in the absence of any shared RF and in the Appendix we finally address the case when no local calibration of measurement devices is ensured.

First, we notice that defining $\vec{a}_i$, $\vec{b}_i^A$, $\vec{b}_i^C$, and $\vec{c}_i$ as the measurement vectors associated to A_i, B_i^A, B_i^C, and C_i, the bilocality parameter $\mathcal{B}$ can be written as

$$\mathcal{B} = \tfrac{1}{2}\sqrt{\left|(\vec{a}_0 + \vec{a}_1)\cdot T_{\varrho_{AB}}\vec{b}_0^A\right| \left|\vec{b}_0^C \cdot T_{\varrho_{BC}}(\vec{c}_0 + \vec{c}_1)\right|} + \tfrac{1}{2}\sqrt{\left|(\vec{a}_0 - \vec{a}_1)\cdot T_{\varrho_{AB}}\vec{b}_1^A\right| \left|\vec{b}_1^C \cdot T_{\varrho_{BC}}(\vec{c}_0 - \vec{c}_1)\right|}, \qquad (3)$$

where the matrix $T_{\varrho_{AB}}$ has components $(t_{\varrho_{AB}})_{ij} = \mathrm{Tr}[\varrho_{AB}\,\sigma_i \otimes \sigma_j]$, and similarly for $T_{\varrho_{BC}}$. Equation (3) makes clear that the value of $\mathcal{B}$ is simply given by the Bloch sphere geometry between the vectors $\vec{a}_i$ and $\vec{b}_j^A$ and between $\vec{c}_i$ and $\vec{b}_j^C$. This implies that even if A and B^A share a reference frame which is different from the one shared between C and B^C (that is, even though stations A and C do no share a common RF) we can still obtain maximum violation of (1). This scenario can be of particular experimental interest when two different and independent channels are used to implement the calibration between the A and B^A and C and B^C measurement devices. However, it still depends on the assumption that no internal calibration between B^A and B^C is taking place.

A more satisfactory situation from the device-independent perspective is one where only A and B^A share a common reference frame, thus guaranteeing that no correlation will be established between A and C. To tackle this case let us consider $\varrho_{AB} = \varrho_{BC} = |\psi^-\rangle\langle\psi^-|$ and $A_x = [\sigma_z + (-1)^x\sigma_x]/\sqrt{2}$, $B_y^A = y\sigma_x + (1-y)\sigma_z$. From Eq. (3) one can show that if C and B^C perform three different measurements belonging to an orthogonal triad ($\{\vec{c}_j\}$ or $\{\vec{b}_k\}$), then the

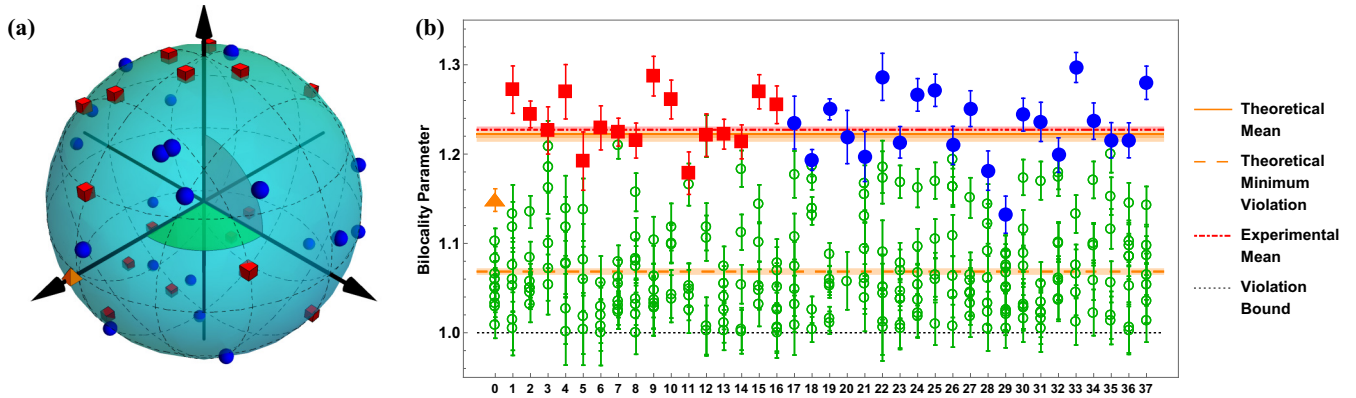

FIG. 4. Experimental test of bilocality with random reference frames between stations B^C and C. (a) Distribution on the Bloch sphere of the performed unitaries for all the experimental points. Red cubes represent points chosen with a uniform pseudorandom distribution, while blue spheres represent random numbers changed for each event acquisitions. The orange pyramid depicts the identity unitary. (b) Amount of violation for all the different randomized unitaries. Given a unitary transformation U_i, green empty circles show the parameter $\mathcal{B}$ for those inequalities [out of 81, considering the different settings and symmetries of (1)] which violate the bilocality condition, except for the maximal violation which is represented with an orange triangle, red squares, or blue disks (corresponding, respectively, to the pyramid, cubes, and spheres of panel (a). Error bars indicate one standard deviation of uncertainty, due to Poissonian statistics. The orange straight (dashed) line shows the theoretical mean (minimum) violation expected for the maximum points (orange triangle, red squares, and blue disks) considering our subset of unitaries, while the red dot-dashed line represents their experimental mean value. The shaded areas display one standard deviation of uncertainty, both for the experimental mean value and for the theoretical expectations due to the experimental estimation of noise. The black dotted line indicates the bilocality violation bound.

following statement holds:

$$\begin{aligned}&\forall \text{ RFs between } C \text{ and } B^C, \quad \exists \vec{c}_\gamma\ \vec{c}_{\gamma'} \in \{\vec{c}_j\}\\ &\text{and}\ \ \vec{b}^C_{\beta_C}\ \vec{b}^C_{\beta'_C} \in \{\vec{b}^C_k\}\ \ \text{such that}\\ &\mathcal{B}\big(\vec{c}_\gamma,\vec{c}_{\gamma'},\vec{b}^C_{\beta_C},\vec{b}^C_{\beta'_C}\big) \geqslant \sqrt[4]{2} \sim 1.19, \end{aligned} \tag{4}$$

where $\{\vec{c}_j\}$ and $\{\vec{b}^C_k\}$ define orthonormal triads.

Proof. If $\varrho_{AB} = \varrho_{BC} = |\psi^-\rangle\langle\psi^-|$ and $A_x = (\sigma_z + (-1)^x\sigma_x)/\sqrt{2}$, $B^A_y = y\sigma_x + (1-y)\sigma_z$, from Eq. (3) of the text we get

$$\begin{aligned}\mathcal{B} &= \frac{\sqrt[4]{2}}{2}\Big(\sqrt{|-\vec{b}^C_0\cdot(\vec{c}_0+\vec{c}_1)|}+\sqrt{|-\vec{b}^C_1\cdot(\vec{c}_0-\vec{c}_1)|}\Big)\\ &= \frac{\sqrt[4]{2}}{2}\big(\sqrt{|E_{00}+E_{10}|}+\sqrt{|E_{11}-E_{01}|}\big),\end{aligned} \tag{5}$$

where we introduced the correlator $E_{jk} = -\vec{c}_j\cdot\vec{b}^C_k$. Let C and B^C perform three different measurements belonging to an orthogonal triad ($\{\vec{c}_j\}$ or $\{\vec{b}_k\}$). It was shown [32] that in this scenario two pairs of measurements exist such that the following inequalities hold:

$$\begin{aligned}E_{00}+E_{10} &\geqslant 1,\\ E_{11}-E_{01} &\geqslant 1,\end{aligned} \tag{6}$$

leading to

$$\mathcal{B} = \frac{\sqrt[4]{2}}{2}\big(\sqrt{|E_{00}+E_{10}|}+\sqrt{|E_{11}-E_{01}|}\big) \geqslant \sqrt[4]{2}. \tag{7}$$

■

This statement shows thus that it is always possible to observe a bilocality violation regardless of the RFs chosen in stations C and B^C, with a minimum value given by $\mathcal{B}_{\min} \geqslant \sqrt[4]{2} \sim 1.19$.

We experimentally addressed this point by using a HWP followed by a liquid crystal on the path leading to station C. These two elements work as a black box which allows us to rotate one of the two qubits all over its Bloch sphere, before it reaches the measurement station. By choosing random settings, it is thus possible to explore a fair subset of all the possible random unitaries which may occur when stations C and B^C do not share a common reference frame (see Appendix B for further details).

Our experimental results are shown in Fig. 4. Red cubes or squares represent random settings chosen accordingly to a uniform distribution over the Bloch sphere, while blue spheres or disks exploit random numbers changed for each event acquisitions. Figure 4(a) shows these shifts on the Bloch sphere, while Fig. 4(b) displays, with red squares and blue disks, the best $\mathcal{B}$ value obtained considering all settings combinations [and symmetries of inequality (1)], for each random unitary. The red dot-dashed line shows the mean value of all these points, which is in good agreement with the theoretical expected value (considering our amount of noise) for our subset of unitaries (orange line). We found at least one value higher than the expected lower bound of $\sqrt[4]{2}$ (corrected with our noise) for all random unitaries, which is represented by the orange dashed line. It is remarkable that, at the cost of performing three instead of two measurements in C and B^C, we can still obtain bilocality violations even when one of the parties shares no RF at all with the other parties.

V. COMPLETE ABSENCE OF SHARED REFERENCES FRAMES

We will analyze now the case when none of the parties share a reference frame with each other. We will start proving

the following statement:

$$\forall \text{ misaligned RFs} \quad \exists \vec{a}_\alpha\ \vec{a}_{\alpha'} \in \{\vec{a}_i\} \text{ and } \vec{b}^A_{\beta_A}\ \vec{b}^A_{\beta'_A} \in \{\vec{b}^A_n\}$$
$$\text{and } \vec{c}_\gamma\ \vec{c}_{\gamma'} \in \{\vec{c}_j\} \text{ and } \vec{b}^C_{\beta_C}\ \vec{b}^C_{\beta'_C} \in \{\vec{b}^C_k\} \text{ such that}$$
$$\mathcal{B}(\vec{a}_\alpha,\vec{a}_{\alpha'},\vec{b}^A_{\beta_A},\vec{b}^A_{\beta'_A},\vec{c}_\gamma,\vec{c}_{\gamma'},\vec{b}^C_{\beta_C},\vec{b}^C_{\beta'_C}) > 1. \tag{8}$$

Proof. Let us define $E^A_{jk} = -\vec{a}_j \cdot \vec{b}^A_k$ and $E^C_{jk} = -\vec{c}_j \cdot \vec{b}^C_k$. The bilocal parameter $\mathcal{B}$ can be expressed as

$$\mathcal{B} = \tfrac{1}{2}\Big(\sqrt{|E^A_{00}+E^A_{10}|}\sqrt{|E^C_{00}+E^C_{10}|} + \sqrt{|E^A_{11}-E^A_{01}|}\sqrt{|E^C_{11}-E^C_{01}|}\Big). \tag{9}$$

We can make use of inequalities (6), which are valid for both E^A_{jk} and E^C_{jk}, in order to show that

$$\begin{aligned}\mathcal{B}^2 &= \tfrac{1}{4}\big(|E^A_{00}+E^A_{10}||E^C_{00}+E^C_{10}| + |E^A_{11}-E^A_{01}||E^C_{11}-E^C_{01}| \\ &\quad + 2\sqrt{|E^A_{00}+E^A_{10}||E^A_{11}-E^A_{01}||E^C_{00}+E^C_{10}||E^C_{11}-E^C_{01}|}\big) \\ &\geqslant \tfrac{1}{4}\big(|E^A_{00}+E^A_{10}| + |E^A_{11}-E^A_{01}| + 2\big) > 1,\end{aligned} \tag{10}$$

where, in the last step, we used the fact that $E^A_{00}+E^A_{10}+E^A_{11}-E^A_{01} > 2$ in the case in which $\{\vec{a}_i\}$ and $\{\vec{b}^A_n\}$ are not aligned reference frames [32]. In the case in which $\{\vec{a}_i\}$ and $\{\vec{b}^A_n\}$ are aligned then it is possible to perform analogous calculations which still prove the theorem under the assumption that $\{\vec{c}_j\}$ and $\{\vec{b}^C_k\}$ are not aligned. We stress that, for random triads, the probability of perfect alignment between all the triads is null. ■

This statement proves that it is still possible to witness a bilocality violation, even if none of the parties shares a common reference frame, at the only cost of performing three measurements per station belonging to an orthogonal triad. Numerical analysis of this case was also performed, and the results are in agreement with the analytical conclusions. All these calculations, however, rely on the presence of local calibration in all of the stations, which allows one to perform orthogonal measurements. Without this assumption one can only have a certain probability of witnessing a bilocality violation, which can be increased performing more measurements per party (see Appendix B).

VI. SUMMARY AND CONCLUSIONS

Generalizations of Bell's theorem for complex networks open novel routes both from fundamental and applied perspectives. Understanding the role of causality within quantum mechanics remains a notoriously thorny issue to which causal structures beyond the one originally devised by Bell can offer new insights [18,21–23]. Further, these more complex networks also have the potential to increase our capabilities to process information in a nonclassical way, since they allow for the emergence of new kinds of quantum nonlocal correlations, in particular the so-called nonbilocality. From the experimental side, these new scenarios introduce new possibilities but also new challenges to be circumvented.

In this work we have taken the next step in the experimental investigation of the bilocality scenario. First, we have shown that one can violate a bilocality inequality using only separable measurements, as opposed to recent experiments [27,28] that require full Bell-state measurements and can only be performed using linear optics if further assumptions are employed, being thus unsatisfactory from a device-independent perspective. Second, we experimentally demonstrated how the presence of shared randomness between Alice and Charlie can be used to mimic quantum nonbilocal correlations with classical mixtures of separable states. This leads to false positives on the violation of bilocality and imposes strict control on the use of shared reference frames between the distant parties involved in the Bell test. Third, in order to deal with this last point, we developed and experimentally verified procedures for witnessing nonbilocality even in the absence of common reference frames. Altogether, we believe these results constitute a building block for the future analysis of the nonclassical correlations arising in complex quantum networks.

ACKNOWLEDGMENTS

G.C. acknowledges Becas Chile and Conicyt for support from a doctoral fellowship. This work was supported by the ERC-Starting Grant 3D-QUEST (3D-Quantum Integrated Optical Simulation; Grant Agreement No. 307783), the Brazilian Ministries MEC and MCTIC, and the FQXi Fund.

APPENDIX A: GENERATING SEPARABLE STATES

We generate the two states $\varrho_{AB} = \varrho_{BC} = (|HH\rangle\langle HH| + |VV\rangle\langle VV|)/2$ setting the compensation HWPs placed after the beta barium borate crystals to 0°. Indeed, in this way, a decoherence effect can be exploited in order to destroy the entanglement between the photons. This walk-off effect separates the H and V polarizations in two different paths, which can be taken into account by considering an additional path degree of freedom ζ for the photons, which is not experimentally witnessed. In the case where the walk-off is compensated, the states ϱ_{AB} and ϱ_{CB} will be

$$\varrho_{XB} = \mathrm{Tr}_\zeta[|\psi^-\rangle|\zeta_1\ \zeta_1\rangle\langle\psi^-|\langle\zeta_1\ \zeta_1|] = |\psi^-\rangle\langle\psi^-|, \tag{A1}$$

where X may represent either A or C. On the other hand, setting the compensation HWP of photons 1 and 4 to 0°, we have

$$\begin{aligned}|\eta\rangle &\equiv \frac{1}{\sqrt{2}}(|HH\rangle|\zeta_1\ \zeta_1\rangle - |VV\rangle|\zeta_2\ \zeta_1\rangle), \\ \varrho_{XB} &= \mathrm{Tr}_\zeta[|\eta\rangle\langle\eta|] = \tfrac{1}{2}(|HH\rangle\langle HH| + |VV\rangle\langle VV|).\end{aligned} \tag{A2}$$

The initial quantum state is thus in the form $\varrho_{ABC} = \varrho_{AB} \otimes \varrho_{BC}$ where

$$\varrho_{AB} = \varrho_{BC} = \frac{\sqrt{v}}{2}(|HH\rangle\langle HH| + |VV\rangle\langle VV|) + (1-\sqrt{v})\frac{\mathbb{I}}{4}, \tag{A3}$$

which takes into account the presence of white noise.

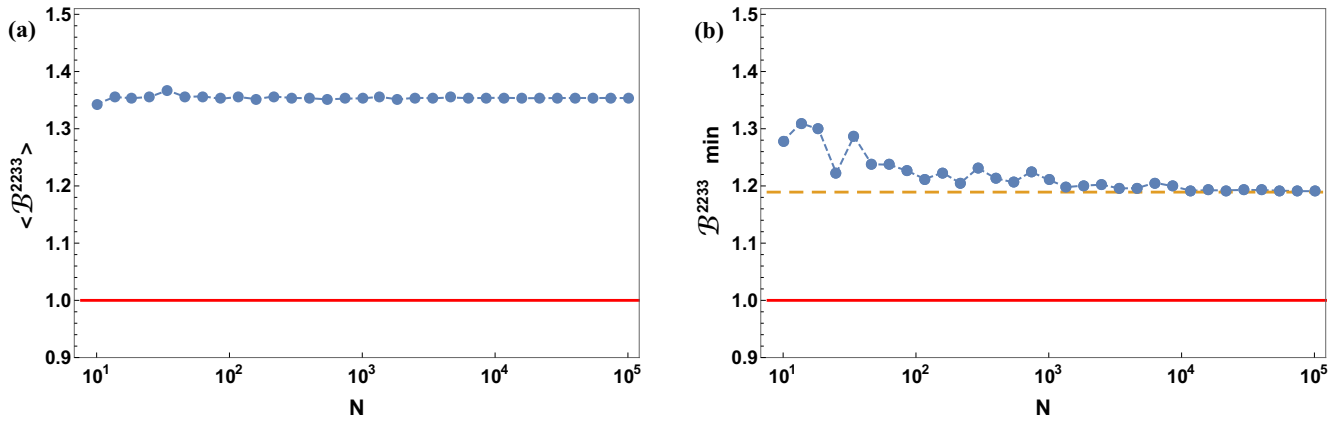

FIG. 5. Numerical analysis of the case when only A and B^A have a common reference frame. (a), (b) Mean (minimum) violation obtained for a growing population of N random misaligned frames. Each point refers to a population which is totally independent from the other ones. The red line shows the violation bound (1.0), while the orange dashed line shows the minimum bound of $\sqrt[4]{2}$ derived in (7).

APPENDIX B: NOISE ESTIMATION

We defined the noise parameter $0 \leqslant V \leqslant 1$, by assuming that the noise which can be present in our experimental realization acts as a generic white noise (i.e., isotropic depolarization). Indeed, if one considers the two Werner states

$$\varrho_{AB} = v_{AB}|\psi^-\rangle\langle\psi^-| + (1 - v_{AB})\frac{\mathbb{I}}{4},$$
$$\varrho_{BC} = v_{BC}|\psi^-\rangle\langle\psi^-| + (1 - v_{BC})\frac{\mathbb{I}}{4}, \tag{B1}$$

instead of two singlet states, then the expected bilocality parameter becomes $\mathcal{B}_{\text{expt}} = V\mathcal{B}_{\text{theor}}$, where $V = \sqrt{v_{AB}v_{BC}}$.

We then took into account the experimental bilocality violation that we obtained (Sec. II of the main text) in the case where a common reference frame for all parties was present. This led to the estimation

$$V = \frac{\mathcal{B}_{\text{expt}}}{\mathcal{B}_{\text{theor}}} = \frac{(1.2712 \pm 0.0042)}{\sqrt{2}} = 0.8989 \pm 0.0030. \tag{B2}$$

APPENDIX C: NUMERICAL SIMULATIONS

1. Shared reference frame between Alice and Bob

We will provide further insight on the first case discussed in the main text, the one when only A and B^A share a reference frame. Let us call $\mathcal{B}^{2233}$ the bilocality parameter for the case where A and B^A perform two measurements, while C and B^C can perform three measurements belonging to an orthogonal triad. In order to perform numerical simulations, one has to consider that a generic rotation in a three-dimensional space needs three parameters to be identified (two for the choice of a rotation axis and one for the angle of rotation). Equivalently we can consider, without loss of generality [31], the two frames

$$\begin{aligned}
x^{BC} &= (\sin\beta^C, -\cos\beta^C, 0),\\
y^{BC} &= (\cos\beta^C, \sin\beta^C, 0),\\
z^{BC} &= (0,0,1),\\
x^{C} &= (\sin\gamma_1\cos\gamma_2, -\cos\gamma_1, -\sin\gamma_1\sin\gamma_2),\\
y^{C} &= (\cos\gamma_1\cos\gamma_2, \sin\gamma_1, -\cos\gamma_1\sin\gamma_2),\\
z^{C} &= (\sin\gamma_2, 0, \cos\gamma_2),
\end{aligned} \tag{C1}$$

We can then analyze all the combinations of two measurements for C and two for B^C and, for each random value of β^C, γ_1, and γ_2, we can take the one which maximizes $\mathcal{B}^{2233}$. We performed several independent runs, with a growing population N of random settings, leading to Fig. 5. For a population of 10^5 random cases we obtained a mean value (for the maximum violation, considering all combinations of settings and the symmetries of the bilocality inequality) of $\langle\mathcal{B}^{2233}\rangle \sim 1.345$, while from Fig. 5(b) it is evident that the lower bound is given by $\sqrt[4]{2}$.

In our experimental setup we are able only to explore a subset of the random rotations which may occur without the presence of a shared reference frame between C and B^C. We indeed are able to randomly rotate one of the two entangled qubits all over its Bloch sphere, leading to the two triads

$$\begin{aligned}
x^{BC}_{\text{subset}} &= (1,0,0),\\
y^{BC}_{\text{subset}} &= (0,1,0),\\
z^{BC}_{\text{subset}} &= (0,0,1),\\
x^{C}_{\text{subset}} &= (\sin\gamma_1\cos\gamma_2, -\cos\gamma_1, -\sin\gamma_1\sin\gamma_2),\\
y^{C}_{\text{subset}} &= (\cos\gamma_1\cos\gamma_2, \sin\gamma_1, -\cos\gamma_1\sin\gamma_2),\\
z^{C}_{\text{subset}} &= (\sin\gamma_2, 0, \cos\gamma_2).
\end{aligned}$$

This subset of random unitaries depends only on two parameters (γ_1 and γ_2) and can be represented by a surface in a three-dimensional space (Fig. 6). We evaluated the mean violation for this case by numerically integrating this surface, obtaining $\langle\mathcal{B}^{2233}_{\text{subset}}\rangle \sim 1.359$ and a lower violation of $\sqrt[4]{2}$.

These results indicate, with good confidence, that the subset of random unitaries which was experimentally explored is a fair sample of the general random rotations set that may occur without a shared reference frame between C and B^C. Indeed, the numerical simulations show that the mean value expected for our experimental subset of unitaries is given by $\langle\mathcal{B}_{\text{subset}}\rangle \sim 1.359$, quite close to the mean value of $\langle\mathcal{B}\rangle \sim 1.345$ obtained when exploring the whole set of unitary transformations. Moreover both sets are bounded by the lower value of $\sqrt[4]{2}$, thus reinforcing that our experimental setup provides a good sampling of random unitaries.

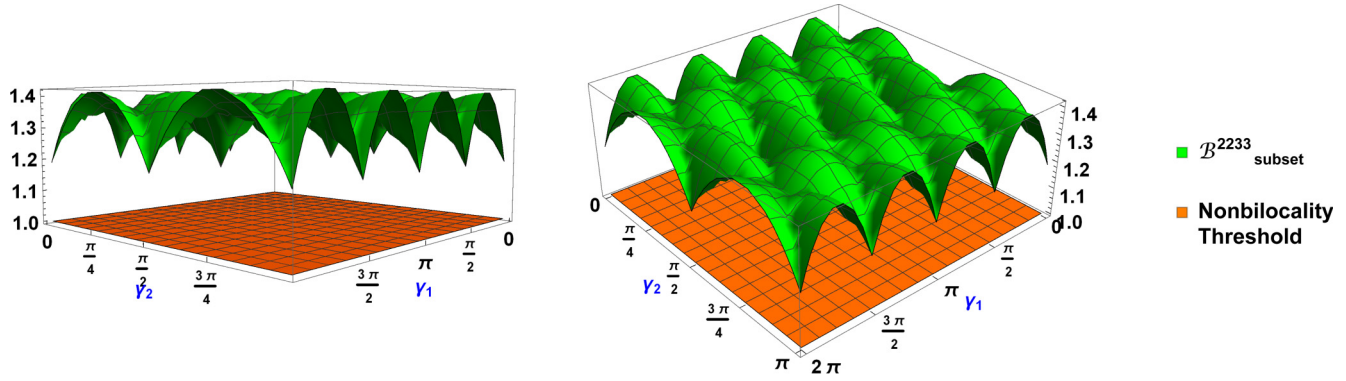

FIG. 6. Numerical analysis of the case $\mathcal{B}^{2233}$ with our experimental subset of random unitaries. The green surface displays $\mathcal{B}^{2233}_{\text{subset}}$ for all the possible values of γ_1 and γ_2, while the orange plane shows the nonbilocality threshold.

All these simulations were derived adopting a uniform distribution for the rotation parameters. Although this is not the most general distribution, we believe it is the most suitable to model the experimental case.

In Fig. 4 of the main text we presented our experimental data. It can be noticed that the orange triangle (corresponding to the identity transformation) exhibits a minimal violation of the bilocality inequality. In order to have a maximal violation (instead of a minimum point) in correspondence to the identity transformation, it is necessary to perform the measurements triad $\{\sigma_x,\sigma_y,\sigma_z\}$ in station B^C and $\{(\sigma_x+\sigma_z)/\sqrt{2},\sigma_y,(\sigma_x-\sigma_z)/\sqrt{2}\}$ in station C (or vice versa). However, we considered a case where there is no clue at all about the possible reference frames' shift, and all rotations have equal probability. In this situation, the most reasonable choice was performing the three orthogonal triads $\{\sigma_x,\sigma_y,\sigma_z\}$ in both stations, also lowering the experimental demands.

2. No shared reference frames at all

Numerical analysis of this case was also performed. This time we have six independent variables associated to the relative shifts between A,B^A and C,B^C, analogously to the previous case. We performed several independent simulations, testing an increasing population of N random shifts. Our conclusions are shown in Fig. 7. Figure 7(a) shows the clear convergence of the mean violation to the value of $\langle\mathcal{B}^{3333}\rangle \sim 1.297$, while Fig. 7(b) gives reasonable evidence of the asymptotic lower bound $\min(\mathcal{B}^{3333}) = 1$. This asymptotic bound is, indeed, exactly what we expect considering that the inequality (10) is not strict anymore in the case in which all reference frames are aligned.

3. Absence of local calibration

We numerically studied the case in which neither shared reference frames nor local calibration are ensured. We analyzed the cases when stations A and C perform two, three, or four measurements, considering each time a population of $N = 2\times10^5$ runs. Figure 8(a) shows the probability density associated to a value of $\mathcal{B}$. This function is obtained grouping the results of the N runs in 200 bins dividing the interval $0 \leqslant \mathcal{B} \leqslant \sqrt{2}$. Curves with different colors refer to an increasing number of measurements performed in stations A and C.

Figure 8(b) shows instead the variation of the violation probability with respect to the noise parameter $V = \sqrt{v_{AB}v_{BC}}$. This figure is obtained integrating the probability densities of Fig. 8(a) from $1/V$ to $\sqrt{2}$. As we can see, increasing the number of measurements quickly makes the violation stronger

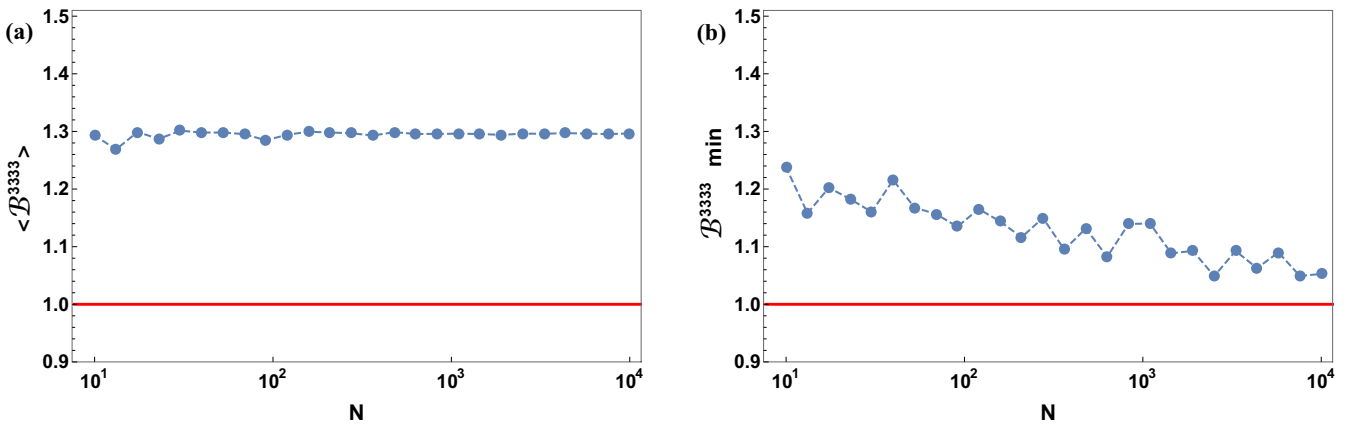

FIG. 7. Numerical analysis of the case when none of the parties have a common reference frame. (a),(b) Mean (minimum) violation obtained for a growing population of N random misaligned frames. Each point refers to a population which is totally independent from the other ones. The red line shows the violation bound (1.0).

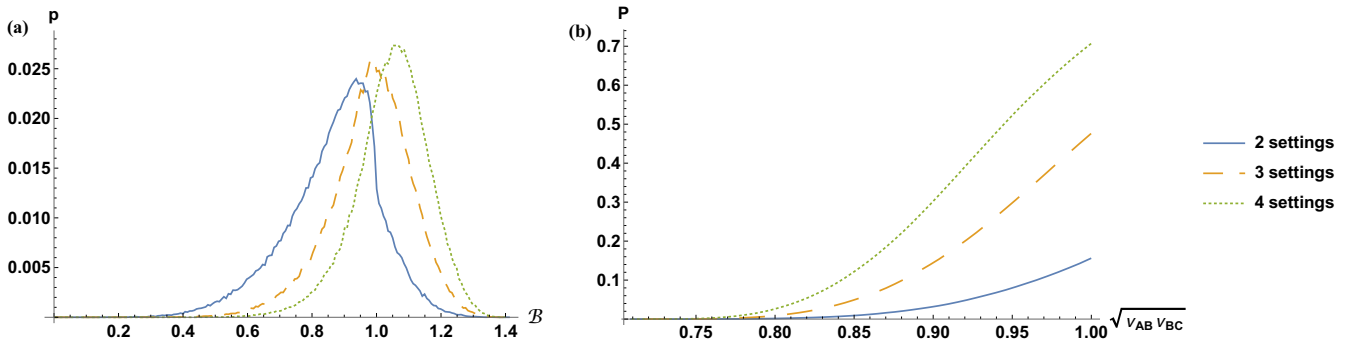

FIG. 8. Numerical analysis of the case when no local calibration is ensured. (a) Probability density of obtaining a value $\mathcal{B}$. Different curves are related to an increasing number of settings (2,3,4) performed in stations A and C. (b) Probability violation with respect to visibility of the Werner states ϱ_{AB} and ϱ_{BC} for the same cases.

to noise. This scheme, however, relies on the exploitation of a higher number of measurements in stations A and C. It is reasonable, however, to guess that increasing also the measurements performed in substations B^A and B^C, a stronger resistance of violation probability against noise can be obtained.

[1] J. S. Bell, On the Einstein—Podolsky—Rosen paradox, Physics **1**, 195 (1964).

[2] N. Brunner, D. Cavalcanti, S. Pironio, V. Scarani, and S. Wehner, Rev. Mod. Phys. **86**, 419 (2014).

[3] B. Hensen, H. Bernien, A. E. Dréau, A. Reiserer, N. Kalb, M. S. Blok, J. Ruitenberg, R. F. L. Vermeulen, R. N. Schouten, C. Abellán *et al.*, Nature (London) **526**, 682 (2015).

[4] L. K. Shalm, E. Meyer-Scott, B. G. Christensen, P. Bierhorst, M. A. Wayne, M. J. Stevens, T. Gerrits, S. Glancy, D. R. Hamel, M. S. Allman, K. J. Coakley, S. D. Dyer, C. Hodge, A. E. Lita, V. B. Verma, C. Lambrocco, E. Tortorici, A. L. Migdall, Y. Zhang, D. R. Kumor *et al.*, Phys. Rev. Lett. **115**, 250402 (2015).

[5] M. Giustina, M. A. M. Versteegh, S. Wengerowsky, J. Handsteiner, A. Hochrainer, K. Phelan, F. Steinlechner, J. Kofler, J. A. Larsson, C. Abellan, W. Amaya, V. Pruneri, M. W. Mitchell, J. Beyer, T. Gerrits, A. E. Lita, L. K. Shalm, S. W. Nam, T. Scheidl, R. Ursin *et al.*, Phys. Rev. Lett. **115**, 250401 (2015).

[6] C. Branciard, N. Gisin, and S. Pironio, Phys. Rev. Lett. **104**, 170401 (2010).

[7] C. Branciard, D. Rosset, N. Gisin, and S. Pironio, Phys. Rev. A **85**, 032119 (2012).

[8] T. Fritz, New J. Phys. **14**, 103001 (2012).

[9] A. Tavakoli, P. Skrzypczyk, D. Cavalcanti, and A. Acín, Phys. Rev. A **90**, 062109 (2014).

[10] R. Chaves, R. Kueng, J. B. Brask, and D. Gross, Phys. Rev. Lett. **114**, 140403 (2015).

[11] C. J. Wood and R. W. Spekkens, New J. Phys. **17**, 033002 (2015).

[12] R. Chaves, Phys. Rev. Lett. **116**, 010402 (2016).

[13] D. Rosset, C. Branciard, T. J. Barnea, G. Pütz, N. Brunner, and N. Gisin, Phys. Rev. Lett. **116**, 010403 (2016).

[14] A. Tavakoli, Phys. Rev. A **93**, 030101 (2016).

[15] M. Ringbauer, C. Giarmatzi, R. Chaves, F. Costa, A. G. White, and A. Fedrizzi, Sci. Adv. **2**, e1600162 (2016).

[16] E. Wolfe, R. W. Spekkens, and T. Fritz, arXiv:1609.00672.

[17] M. S. Leifer and R. W. Spekkens, Phys. Rev. A **88**, 052130 (2013).

[18] J. Henson, R. Lal, and M. F. Pusey, New J. Phys. **16**, 113043 (2014).

[19] E. G. Cavalcanti and R. Lal, J. Phys. A: Math. Theor. **47**, 424018 (2014).

[20] C. Brukner, Nat. Phys. **10**, 259 (2014).

[21] R. Chaves, C. Majenz, and D. Gross, Nat. Commun. **6**, 5766 (2015).

[22] F. Costa and S. Shrapnel, New J. Phys. **18**, 063032 (2016).

[23] T. Fritz, Commun. Math. Phys. **341**, 391 (2016).

[24] D. Horsman, C. Heunen, M. F. Pusey, J. Barrett, and R. W. Spekkens, arXiv:1607.03637.

[25] N. Sangouard, C. Simon, H. de Riedmatten, and N. Gisin, Rev. Mod. Phys. **83**, 33 (2011).

[26] M. Zukowski, A. Zeilinger, M. A. Horne, and A. K. Ekert, Phys. Rev. Lett. **71**, 4287 (1993).

[27] G. Carvacho, F. Andreoli, L. Santodonato, M. Bentivegna, R. Chaves, and F. Sciarrino, Nat. Commun. **8**, 14775 (2017).

[28] D. J. Saunders, A. J. Bennet, C. Branciard, and G. J. Pryde, Sci. Adv. **3**, e1602743 (2017).

[29] J. Pearl, *Causality* (Cambridge University Press, Cambridge, UK, 2009).

[30] Y.-C. Liang, N. Harrigan, S. D. Bartlett, and T. Rudolph, Phys. Rev. Lett. **104**, 050401 (2010).

[31] J. J. Wallman and S. D. Bartlett, Phys. Rev. A **85**, 024101 (2012).

[32] P. Shadbolt, T. Vértesi, Y.-C. Liang, C. Branciard, N. Brunner, and J. L. O'Brien, Sci. Rep. **2**, 470 (2012).

[33] V. D'Ambrosio, E. Nagali, S. P. Walborn, L. Aolita, S. Slussarenko, L. Marrucci, and F. Sciarrino, Nat. Commun. **3**, 961 (2012).

[34] J. B. Brask, R. Chaves, and N. Brunner, Phys. Rev. A **88**, 012111 (2013).

[35] Z. Wang, C. Zhang, Y. F. Huang, B. H. Liu, C. F. Li, and G. C. Guo, Phys. Rev. A **93**, 032127 (2016).

[36] N. Lütkenhaus, J. Calsamiglia, and K.-A. Suominen, Phys. Rev. A **59**, 3295 (1999).

[37] F. Andreoli, G. Carvacho, L. Santodonato, R. Chaves, and F. Sciarrino, arXiv:1702.08316.